Identification of the Binding Surface on Cdc42Hs for p21-Activated Kinase†

Wei Guo,‡ Michael J. Sutcliffe,§ Richard A. Cerione,‡ and Robert E. Oswald*,‡

Department of Molecular Medicine, Cornell University, Ithaca, New York 14853, and Department of Chemistry, Leicester University, Leicester, LE1 7RK, U.K.

Received June 8, 1998; Revised Manuscript Received August 7, 1998

ABSTRACT: The Ras superfamily of GTP-binding proteins is involved in a number of cellular signaling events including, but not limited to, tumorigenesis, intracellular trafficking, and cytoskeletal organization. The Rho subfamily, of which Cdc42Hs is a member, is involved in cell morphogenesis through a GTPase cascade which regulates cytoskeletal changes. Cdc42Hs has been shown to stimulate DNA synthesis as well as to initiate a protein kinase cascade that begins with the activation of the p21-activated serine/threonine kinases (PAKs). We have determined previously the solution structure of Cdc42Hs [Feltham et al. (1997) *Biochemistr*y 36, 8755−8766] using NMR spectroscopy. A minimal-binding domain of 46 amino acids of PAK was identified (PBD46), which binds Cdc42Hs with a K_D of approximately 20 nM and inhibits GTP hydrolysis. The binding interface was mapped by producing a fully deuterated sample of ^{15}N-Cdc42Hs bound to PBD46. A ^{1}H,^{15}N-NOESY-HSQC spectrum demonstrated that the binding surface on Cdc42Hs consists of the second β-strand (β2) and a portion of the loop between the first α-helix (α1) and β2 (switch I). A complex of PBD46 bound to ^{15}N-Cdc42Hs·GMPPCP exhibited extensive chemical shift changes in the ^{1}H,^{15}N-HSQC spectrum. Thus, PBD46 likely produces structural changes in Cdc42Hs which are not limited to the binding interface, consistent with its effects on GTP hydrolysis. These results suggest that the kinase-binding domain on Cdc42Hs is similar to, but more extensive than, the c-Raf-binding domain on the Ras antagonist, Rap1 [Nassar et al. (1995) *Nature 375*, 554−560)].

A superfamily of low molecular weight G-proteins, for which the Ras proteins serve as prototypes, is involved in many biological pathways including cell cycle progression, cytoskeletal organization, protein trafficking, and secretion (*1*). The most intensively studied members of this superfamily are the Ras subfamily proteins which play a major role in cell growth, differentiation, and possibly, apoptosis. The Rho subfamily, however, has been shown to control various cellular signaling pathways leading to changes in cell morphology and polarity, as well as increased DNA synthesis and cell cycle progression (*2*−*4*). Recent experiments suggest that Cdc42Hs, a member of Rho subfamily, may work closely with Ras to provide a full complement of cell growth regulatory events (*5*). The evidence includes the regulation of Cdc42Hs by the oncogenic protein Dbl (*6, 7*) and the fact that activated mutants of Cdc42Hs can transform cells (*5, 8*).

During the past several years, a variety of Cdc42Hs target proteins have been identified including the p85 subunit of the PI3 kinase (*9*), the Wiscott−Aldrich syndrome protein [WASP (*10*)], the IQ-GAP molecules (*11, 12*), the ACK tyrosine kinase (*13, 14*), and members of the PAK[1] family of serine/threonine kinases (*15, 16*). Although these potential Cdc42Hs signaling responses are assumed to be coordinated, how these molecules interact with each other and how these interactions are regulated remains unknown. Recent studies of the interaction between Cdc42Hs and Rac with PAKs (*17*−*21*) support the idea that activation of PAK by Cdc42Hs/Rac initiates a protein kinase cascade that leads to the nucleus and culminates in the activation of two nuclear MAP kinases, JNK1 and p38. This kinase cascade pathway is similar to a pathway in *Saccharomyces cerevisiae*, where STE20 (the PAK homolog) initiates a kinase cascade that results in the activation of the MAP kinase Fus3/Kss1 (*22*) and resembles the Ras-signaling pathway that begins with the Raf serine/threonine kinase and culminates in the activation of the nuclear MAP kinase Erk (*23*). However, while the main role of Ras appears to be to recruit Raf to the membrane where it then becomes activated, Cdc42Hs or Rac is absolutely essential for the stimulation of PAK activity. Without one or more activated Rho proteins, the PAKs cannot be autophosphorylated and show no kinase activity. Structural studies of the Ras-binding domain on the Ras antagonist, Rap1A, (*24*) reveals that the interaction between the two proteins is mediated by an antiparallel

† Supported by grants from the American Cancer Society and the NIH (R01 GM56233) to R.E.O. W.G. was supported by an NIH predoctoral training grant (T32GM08210). M.J.S. is a Royal Society University Research Fellow.

* To whom correspondence should be addressed. Phone: 1-607-253-3877. Fax: 1-607-253-3659. E-mail: reo1@cornell.edu.

‡ Cornell University.

§ Leicester University.

[1] Abbreviations: DTT, dithiothreitol; EDTA, ethylenediaminetetraacetic acid; GAP, GTPase-activating protein; GDP, guanosine 5′-diphosphate; GMPPCP, β,γ-methylene derivative of GTP; GSH, glutathione (reduced form); GST, glutathione *S*-transferase; GTP, guanosine 5′-triphosphate; HSQC, heteronuclear single quantum correlation; IPTG, isopropyl β-D-thiogalactopyranoside; NMR, nuclear magnetic resonance; NOESY, nuclear Overhauser effect spectroscopy; PAK, p21 activated kinase; PBD, Cdc42Hs binding domain on PAK; PBS, phosphate-buffered saline; PMSF, phenylmethanesulfonyl fluoride; RBD, Ras-binding domain; sNBD, succinimidyl-6-[(7-nitrobenz-2-oxa-1,3-diazol-4-yl)amino]hexanoate; Tris-HCl, tris[hydroxymethyl]-aminomethane hydrochloride.

S0006-2960(98)01352-X CCC: $15.00
Published on Web 09/15/1998

β-sheet formed by strand β2 from RBD (Ras-binding domain) and strand β2 from Rap1A. In contrast to the interaction between Ras and Raf, PAK can decrease the rate of GTP hydrolysis by Cdc42Hs, suggesting that the interaction may be different or more extensive than the Ras-Raf interaction.

Presented here is the delineation of the binding interface on Cdc42Hs for PAK and the backbone chemical shift changes of Cdc42Hs upon binding of a peptide derived from PAK. This peptide encompasses the CRIB (Cdc42/Rac interactive binding) domain, which is also present in WASP and the ACKs and has been identified on the basis of sequence alignment as an important determinant in the binding of Cdc42Hs and Rac (*25*). The binding interface is more extensive than that described for Rap1A-RBD (*24*), and the chemical shift changes encompass a large surface of Cdc42Hs, suggesting that PAK binding has significant effects on the tertiary structure of this GTP-binding protein.

EXPERIMENTAL PROCEDURES

Protein Expression. Cdc42Hs used in these experiments was expressed as a hexa-histidine-tagged protein in *Escherichia coli* strain BL21(DE3) from pET-15b-Cdc42Hs. This expression plasmid was subcloned to contain the N-terminal 181 amino acids (including a glycine, serine, and histidine before the starting methionine) from the original pGEX-Cdc42Hs expression plasmid (*26*) to improve the yield and to remove the unstructured C-terminal tail (*27*). For samples labeled homogeneously with ^{15}N or $^{15}N/^{13}C$, $^{15}NH_4Cl$ and ^{13}C-glucose were substituted for their unlabeled counterparts in the M9 media (*28*). Specifically, a single colony containing plasmid pET-15b-Cdc42Hs was grown for 8 h in 5 mL of LB containing 50 μg/mL ampicillin (this concentration of ampicillin was maintained in all media). This 5 mL culture was washed twice with 5 mL of fresh 2×M9 unlabeled media and transferred to 200 mL of 2×M9 unlabeled media to grow 12 h at 37 °C in a shaker flask. The 200 mL culture was then washed twice with 200 mL of 2×M9 unlabeled media, resuspended in 2 L of 2×M9 ^{15}N- or $^{15}N/^{13}C$-labeled media, and grown in a Hi-Density Fermentor (Lab-Line Instrument, Melrose Park, IL) to OD_{560} = 0.7. Cells were harvested 6 h after induction with 0.5 mM IPTG by centrifugation at 10000*g* for 15 min (4 °C) and stored at −70 °C.

Several modifications of this procedure were required to produce $^{15}N,^{2}H$-Cdc42Hs. $^{15}NH_4Cl$ and ^{2}H-sodium acetate were used in the 2×M9 as the sole nitrogen and carbon sources, and 50 μg/mL carbenicillin was used throughout the procedure. A single bacterial colony containing expression plasmid pET-15b-Cdc42Hs was grown in 3 mL of 33% D_2O LB for 12 h at 37 °C in a 15 mL culture tube. An aliquot (100 μL) was then transferred to 3 mL of 67% D_2O LB for an additional 12 h. Finally, 100 μL was transferred to 3 mL of >98% D_2O LB for 12 h. An aliquot (50 μL) of this culture was transferred to 50 mL of >98% D_2O 2×M9 and was grown for 3 days at 37 °C in a shaker flask. This 50 mL culture was then transferred to 2 L of >98% D_2O 2×M9 and grown for 2 days at 37 °C. When OD_{560} = 0.5 was reached, induction began with 0.5 mM IPTG. Cells were harvested after 36 h of induction as described above.

PBD46 was expressed as a GST fusion protein (pGEX-2T-PBD46) in *Escherichia coli* strain BL21(DE3). This expression plasmid was subcloned from the original pET-15b-PBD (*29*) and contained 46 amino acids, including glycine and serine introduced as an N-terminal linker before the PBD sequence. Expression was achieved in the same manner as for Cdc42Hs, except that 4 L of LB medium was used and induction by IPTG began when the medium reached OD_{560} = 1.0 in the fermentor.

Protein Purification. All procedures were performed at 4 °C unless otherwise specified. Frozen cells containing Cdc42Hs were thawed in 100 mL lysis buffer (5 mM imidazole, 500 mM NaCl, 20 mM Tris-HCl, pH 8.0) with 0.1 mM GDP and a cocktail of protease inhibitors (2 μg/mL aprotinin, leupeptin and pepstatin, and 10 μg/mL benzamidine and PMSF). Cells were homogenized using a Teflon-glass homogenizer, and lysozyme and deoxycholic acid were added to 1 mg/mL and 0.8 mg/mL respectively. Cell lysates were incubated for 30 min, followed by the addition of DNase I and $MgCl_2$ to final concentration of 20 μg/mL and 20 mM, respectively. The lysates were then disrupted using a Polytron. The insoluble fraction was removed by centrifugation at 20000*g* for 20 min. The supernatant was applied to an iminodiacetic acid column (15 mL) previously charged with Ni^{2+} and equilibrated with binding buffer (5 mM imidazole, 500 mM NaCl, and 20 mM Tris-HCl, pH 8.0). The column was washed with binding buffer and washing buffer (25 mM imidazole, 500 mM NaCl, and 20 mM Tris-HCl, pH 8.0) and eluted with a 25 to 300 mM imidazole gradient containing 500 mM NaCl and 20 mM Tris-HCl, pH 8.0. Thrombin was added to the pooled Cdc42Hs-GDP (identified by 10% SDS−PAGE) and dialyzed against 4 L of 20 mM Tris-HCl (pH 8.0) for at least 5 h before the addition of 10 μg/mL PMSF to stop the reaction. The mixture (containing Cdc42Hs·GDP, hexa-histidine tag, and thrombin) was loaded on a 15 mL Q-Sepharose column (equilibrated with 20 mM Tris-HCl, pH 8.0), washed with 20 mM Tris-HCl (pH 8.0), and eluted with a 0 to 300 mM NaCl gradient. Cdc42Hs·GDP was the only protein in the mixture that bound to this column. Following elution, Cdc42Hs·GDP was identified by 10% SDS−PAGE, concentrated to 20 mg/mL [Bradford assay (*30*) after correction based on an amino acid analysis (*27*)], and dialyzed against NMR buffer (25 mM NaCl, 5 mM NaH_2PO_4, 5 mM $MgCl_2$, and 1 mM NaN_3, pH 5.5). Exchange of GDP for GMPPCP was performed as described by John et al. (*31*). Cdc42Hs·GMPPCP was further dialyzed extensively in NMR buffer and concentrated to 20 mg/mL.

A supernatant containing GST-PBD46 was extracted from bacteria in the same manner as described for His-Cdc42Hs except that PBS was used as the lysis buffer. The supernatant was mixed with 50 mL of GST Sepharose-4B beads which were equilibrated with PBS. The mixture was poured onto a column, washed with 300 mL of PBS and 100 mL of 20 mM Tris-HCl, pH 8.0. The GST fusion protein was eluted with 10 mM GSH in 20 mM Tris-HCl (pH 8.0), and fractions containing GST-PBD46 (identified by 10% SDS−PAGE) were pooled (~100 mL) and incubated with thrombin for 5 h. The solution was lyophilized, resuspended in 3 mL of H_2O, centrifuged, and loaded on to a Sephacryl S-100 gel filtration column prior equilibrated with 20 mM Tris-HCl and 150 mM NaCl, pH 8.0. Purified PBD46 was eluted, identified by SDS−PAGE, lyophilized, resuspended in 2 mL of H_2O, dialyzed in the NMR buffer described above, and

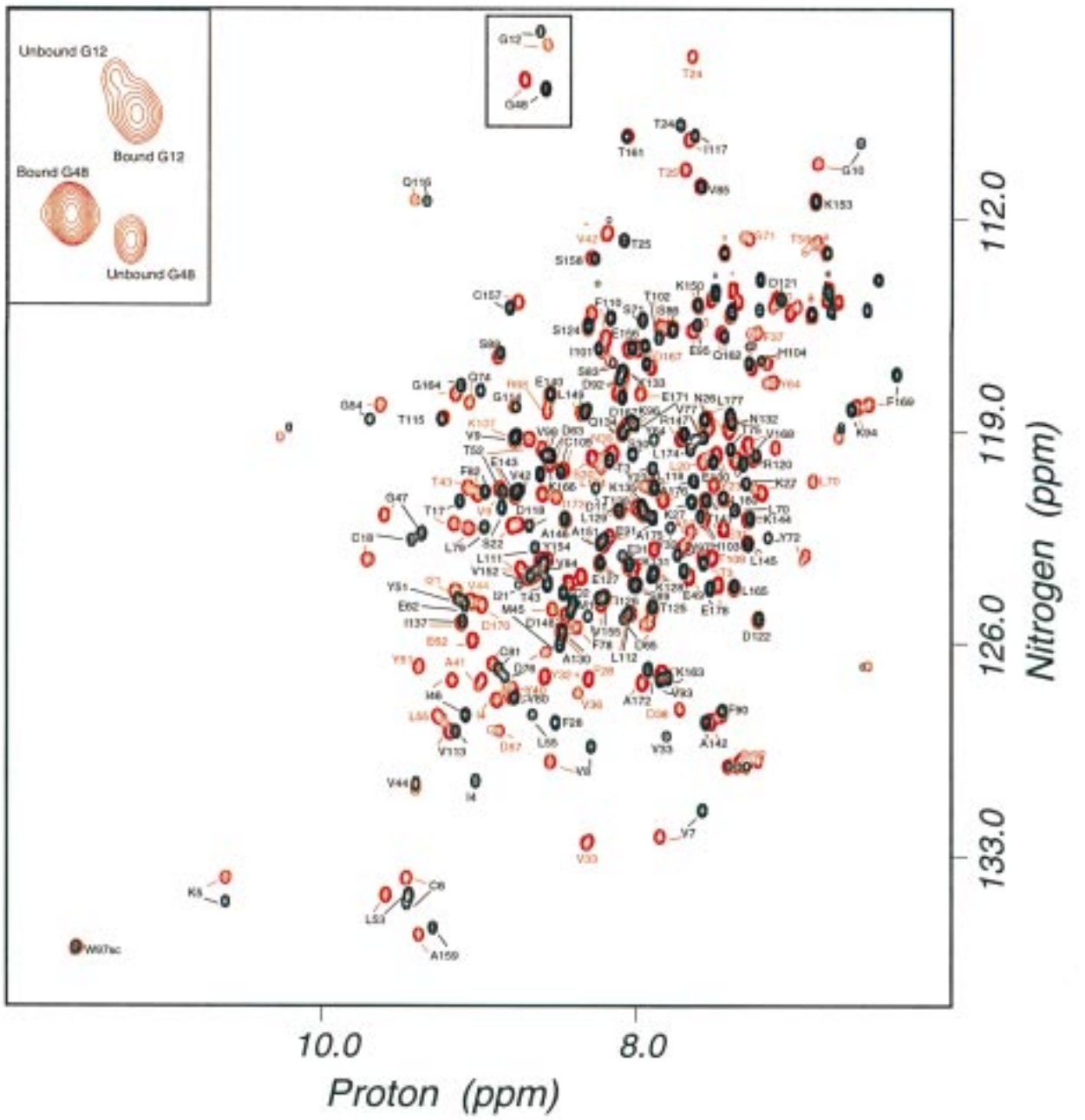

FIGURE 1: The ^{1}H,^{15}N-HSQC spectra of ^{15}N-Cdc42Hs·GMPPCP (black) and ^{15}N-Cdc42Hs·GMPPCP-PBD46 (red) are shown with peaks labeled with assignments. Side-chain glutamine and asparagine correlations are not labeled. Since only Cdc42Hs is uniformly labeled with ^{15}N, only correlations between nitrogen and amide protons on Cdc42Hs are observable. Note: the extensive chemical shift changes between the PBD-bound and PBD-free forms of ^{15}N-Cdc42Hs·GMPPCP. The insert is an enlargement at lower contour levels of a partially bound ^{15}N-Cdc42Hs·GMPPCP preparation showing both bound and unbound peaks, indicating that the complex is in slow exchange.

concentrated to 5 mg/mL. PBD46 and Cdc42Hs·GMPPCP were then mixed (1 mL each of the protein stocks) and incubated at 4 °C overnight. The complex was purified on a Sephacryl S-100 column equilibrated with NMR buffer.

Protein samples used for NMR experiments were supplemented with 10% D_2O. The concentration of ^{15}N-Cdc42Hs·GMPPCP was 1.0 mM, ^{15}N-Cdc42Hs·GMPPCP-PBD46 was 1.0 mM, and ^{15}N,^{2}H-Cdc42Hs·GMPPCP-PBD46 was 0.8 mM. All samples were in NMR buffer at pH 5.5 without pH correction to counter isotope effects.

Binding of PBD46 to Cdc42Hs. A fluorescence reporter group, sNBD, was covalently attached to Lys150 on Cdc42Hs (*32*). sNBD-labeled Cdc42Hs undergoes a characteristic fluorescence decrease when bound to PBD [excitation at 488 nm and emission at 545 nm (*32*)], providing an environment-sensitive probe for monitoring the binding of Cdc42Hs to PBD. Accordingly, 55 nM of sNBD-Cdc42Hs·GTP in NMR buffer was excited at 488 nm, aliquots of concentrated PBD constructs were added, and the fluorescence quenching was monitored. The K_D was determined by nonlinear least-squares fit to the following equation:

$$F = F_i + F_f\left[\frac{(K_D + L_t + R_t) - \sqrt{(K_D + L_t + R_t)^2 - 4R_tL_t}}{2R_t}\right]$$

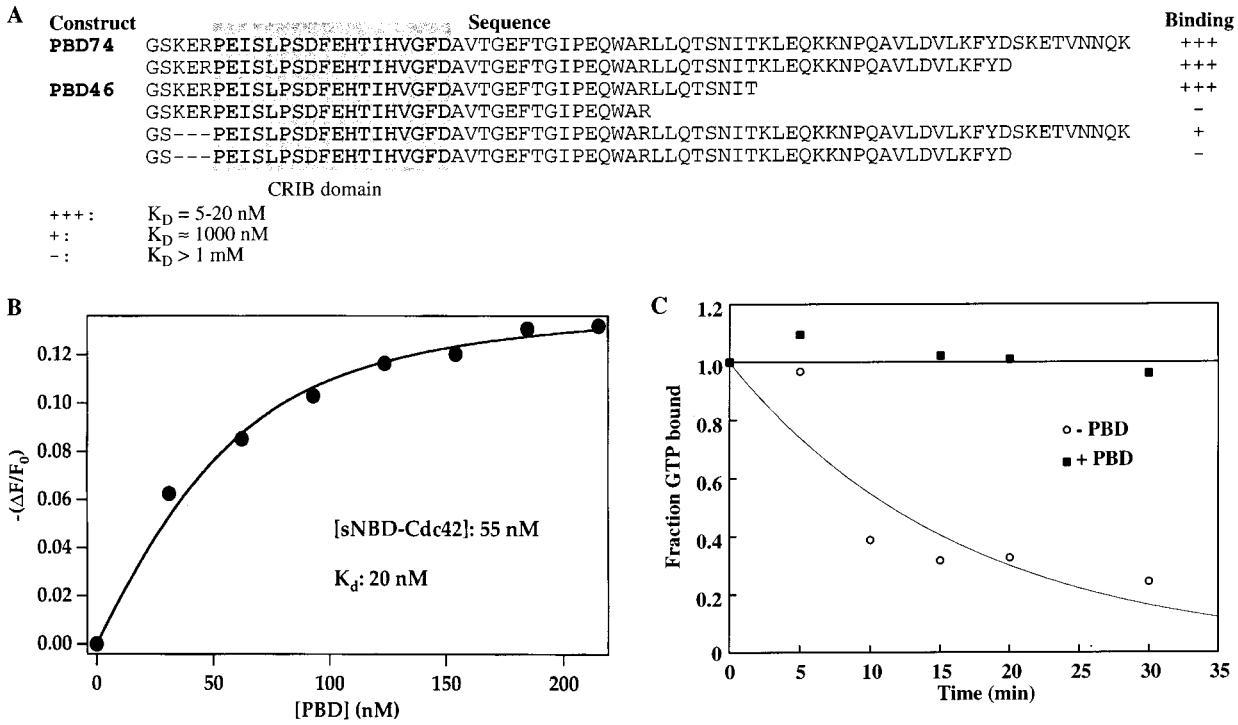

FIGURE 2: Sequence and characterization of PBD46. (A) The amino acid sequences of the PBD constructs tested are shown along with an indication of the affinity of each sequence for Cdc42Hs·GMPPCP based on the sNBD-binding assay. PBD46 was the shortest construct which bound with high affinity. (B) Binding of PBD46 to sNBD-Cdc42Hs·GMPPCP results in a fluorescence decrease upon binding (the *y*-axis represents a decrease in fluorescence intensity). A K_D of 20 nM was calculated as described in the Experimental Procedures. (C) Inhibition of Cdc42Hs-catalyzed GTP hydrolysis by PBD46. In the absence of PBD46, Cdc42Hs hydrolyzed GTP with $t_{1/2}$ of approximately 14 min. In the presence of 10 μM of PBD46, a significant decrease in the rate of ^{32}P release from the GTPase was observed. The curve shown for the GTPase activity in the absence of PBD is a single-exponential fit to the data.

where F is the change in fluorescence over the initial fluorescence ($\Delta F/F_o$), F_i is the initial value of $\Delta F/F_o$, F_f is the final value of $\Delta F/F_o$, L_t is the total concentration of PBD, and R_t is the total concentration of Cdc42Hs.

Measurement of GTPase Activity of Cdc42Hs. The hydrolysis of GTP by Cdc42Hs was measured by monitoring the release of ^{32}P from [γ-^{32}P]GTP bound to Cdc42Hs (*29*). Purified Cdc42Hs (10 μM) was complexed with 7 μM [γ-^{32}P]-GTP (360 000 cpm/pmol) in TEDA buffer (20 mM Tris-HCl, pH 7.5, 10 mM EDTA, 1 mM DTT, and 50 mM NaCl) and 80 μg/mL bovine serum albumin for 20 min at room temperature. To initiate hydrolysis of the bound GTP, aliquots of the Cdc42Hs were then diluted into a reaction mixture containing 25 mM Tris-HCl, pH 7.5, 1.3 mM DTT, 40 mM NaCl, 5 mM $MgCl_2$, 200 μg/mL bovine serum albumin, 100 μM nonradioactive GTP, and either purified PBD46 or control buffer (TEDA buffer, 40% glycerol). Aliquots were filtered on BA-85 nitrocellulose filters (Schleicher and Schuell) and washed under negative pressure. The amount of ^{32}P remaining associated with Cdc42Hs was determined by liquid scintillation counting of the filters.

NMR Spectroscopy. NMR experiments were performed at 25 °C on a Varian Inova 600 spectrometer with a triple resonance pulsed-field gradient probe. Data were collected in the States-TPPI mode (*33, 34*) for quadrature detection. Chemical shifts were referenced as described previously (*27*).

2D Heteronuclear Experiments. 2D ^{1}H,^{15}N heteronuclear single quantum coherence [HSQC (*35*)] spectra were acquired on Cdc42Hs, and Cdc42Hs-PBD46 samples in which Cdc42Hs was homogeneously labeled with ^{15}N.

3D Experiments for Sequential Backbone Assignments. For both ^{15}N,^{13}C-Cdc42Hs·GMPPCP and ^{15}N,^{13}C-Cdc42Hs·GMPPCP-PBD46, an HNCA was collected (HNCA with decoupling of C_β nuclei) as in Yamazaki et al. (*36*) except for the removal of sensitivity enhancement pulses. During t_1, WALTZ-16 decoupling was applied to protons, allowing the removal of T_c (C_α constant time period), and WURST decoupling (*37, 38*) is applied to both the carbonyls and C_β nuclei (*39*). An HN(CO)CA experiment used a nonsensitivity-enhanced version of the pulse sequence in Yamazaki et al. (*40*), except for the addition of SEDUCE decoupling of C_α nuclei during τ_c (in which coupling develops between nitrogen and the carbonyl) and WURST decoupling of C_β nuclei in t_1, as well as WALTZ-16 decoupling of protons in t_1, allowing the removal of T_c (C_α constant time period). An additional series of experiments were used to correlate backbone amides and amide protons to C_β nuclei: HBCB-CACONNH and HNCACB (*41*−*43*).

3D NOESY Experiments. ^{1}H,^{15}N-NOESY-HSQC (*34, 44*) experiments were acquired on ^{15}N-Cdc42Hs·GMPPCP, ^{15}N-Cdc42Hs·GMPPCP-PBD46, ^{15}N,^{2}H-Cdc42Hs·GMPPCP, and ^{15}N,^{2}H-Cdc42Hs·GMPPCP-PBD46 using a pulse sequence which features water suppression by a selective pulse on the water resonance followed by dephasing with a gradient during the mixing period, as well as by a gradient applied while the magnetization of interest is spin-ordered during the final INEPT transfer step.

Processing of NMR Experiments. Data were processed with version 2.3 of Felix software (Molecular Simulations, Inc.) on an SGI Indy workstation, with preprocessing for sensitivity-enhanced experiments (*45*). Data were, in most

cases, zero-filled to double the original number of data points and apodized by convolution with a squared sinebell window function shifted by 60−90°, depending on the relative amount of signal in the data. Linear prediction was sometimes applied during the transformation of this final dimension to increase resolution. Data visualization and spectral assignment utilized the XEASY (*46*) program.

RESULTS AND DISCUSSION

Optimization of Cdc42Hs and PBD Constructs. A complex of full-length ^{15}N-Cdc42Hs (*27*) with a 74 amino acid PBD construct described previously (*16*) gave rise to ^{1}H,^{15}N-HSQC spectra with unacceptably broad lines (data not shown). By removing the flexible C- and N-terminal portions of the original Cdc42Hs construct [note that the original construct contained 9 amino acids that were not native to Cdc42Hs, but remained from the cloning of the cDNA (*27*)], the resulting 178 amino acid protein produced excellent spectra (Figure 1).

The original 74 amino acid PBD construct was found to be unstable due to proteolysis during purification. Therefore, to determine the core binding sequence of PBD, a series of truncation mutants of both the N- and C-termini surrounding the CRIB sequence [Figure 2A (*25*)] was expressed and purified as GST fusion proteins. Following removal of GST by thrombin and purification, binding assays of each peptide to sNBD-labeled Cdc42Hs were performed according to Nomanbhoy et al. (*32*) as described in the Experimental Procedures. Among the constructs tested, PBD46 was the smallest peptide which maintained an affinity for the GTP-bound form of Cdc42Hs close to that of native mPAK-3 (Figure 2B, $K_D = 20$ nM vs 5 nM for the wild-type protein). In addition, like mPAK-3, PBD46 inhibited the hydrolysis of GTP by Cdc42Hs (Figure 2C). As shown in Figure 2C, Cdc42Hs hydrolyzed GTP rapidly ($t_{1/2}$ of approximately 14 min) in the absence of PBD46. However, in the presence of 10 μM of PBD46, no GTP hydrolysis was observed within the time of the experiment. Thus, both the binding affinity and function of the p21-binding domain found in mPAK-3 (*15*, *16*) is preserved in PBD46. As shown in Figure 1, the complex of PBD46 with ^{15}N-Cdc42Hs·GMPPCP produced excellent ^{1}H,^{15}N-HSQC spectra.

Backbone Assignments of Cdc42Hs·GMPPCP and Its Complex with PBD46. The assignments for a full-length construct of Cdc42Hs·GMPPCP have been reported previously (*27*). The truncated form used in the current experiments showed minor chemical shift changes, and the assignments (^{13}C,^{15}N-Cdc42Hs·GMPPCP) were verified using four triple resonance experiments (HNCO, HNCA, HBCBCACONNH, and HNCACB) which provided assignments for all backbone resonances as well as C_β resonances with the exception of several resonances broadened by conformational dynamics on an intermediate time scale [resonances in the P-loop (residues 14−15), switch I (residues 36−41) and switch II (residues 59−61) (*27*)].

As described above, the binding of PBD46 to Cdc42Hs·GMPPCP exhibits high affinity, and HSQC spectra of ^{15}N-Cdc42Hs·GMPPCP partially complexed with PBD46 exhibits peaks arising from both bound and unbound ^{15}N-Cdc42Hs·GMPPCP, indicating that the complex is in slow exchange (Figure 1, inset). As shown in Figure 1, a large

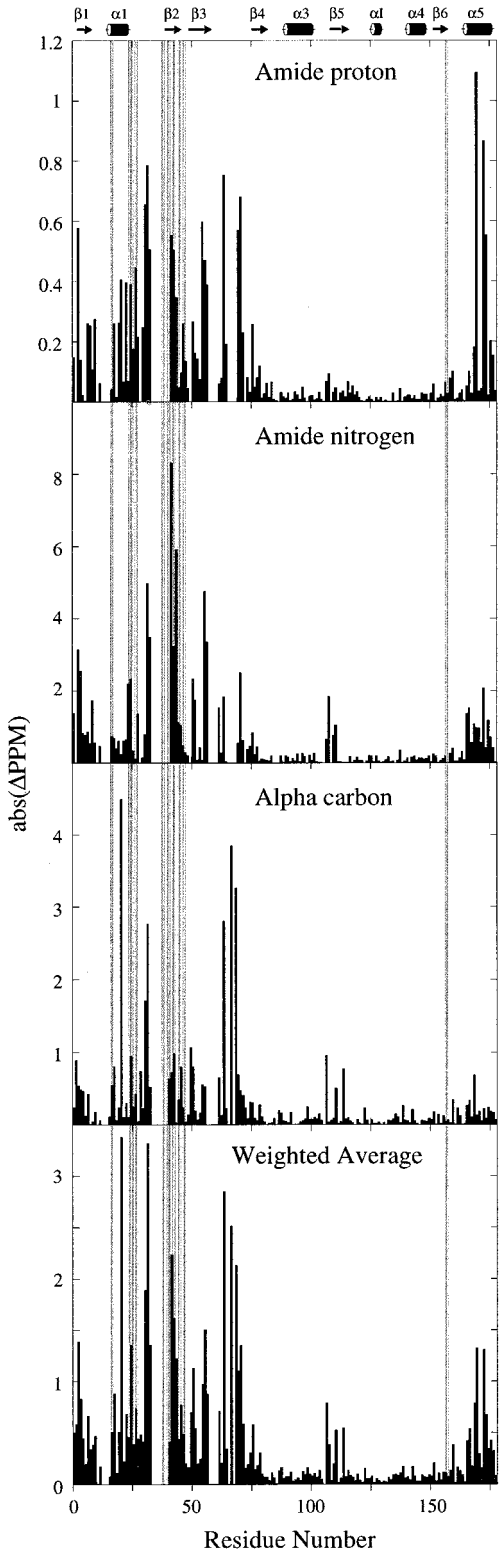

FIGURE 3: Changes in chemical shift as a function of residue number upon Cdc42Hs·GMPPCP binding to PBD46. The changes for the amide proton and amide nitrogen are derived from the ^{1}H,^{15}N-HSQC spectra and the changes in the C_α nuclei are derived from an HNCA spectrum. The weighted average was generated by scaling to the range of chemical shifts in the sample for ^{1}H and ^{15}N nuclei (4.3 and 29.6 ppm, respectively) and to the average chemical shift range for $^{13}C_\alpha$ nuclei [6.6 ppm, calculated from the data in Wishart et al. (*52*)]. The gray bars indicate the residues for which intermolecular contacts have been observed from the NOE experiment shown in Figure 5. Ambiguity due to missing assignments in either the bound or unbound spectra is present for positions 13−15, 35−40, 58−61, and 66−68.

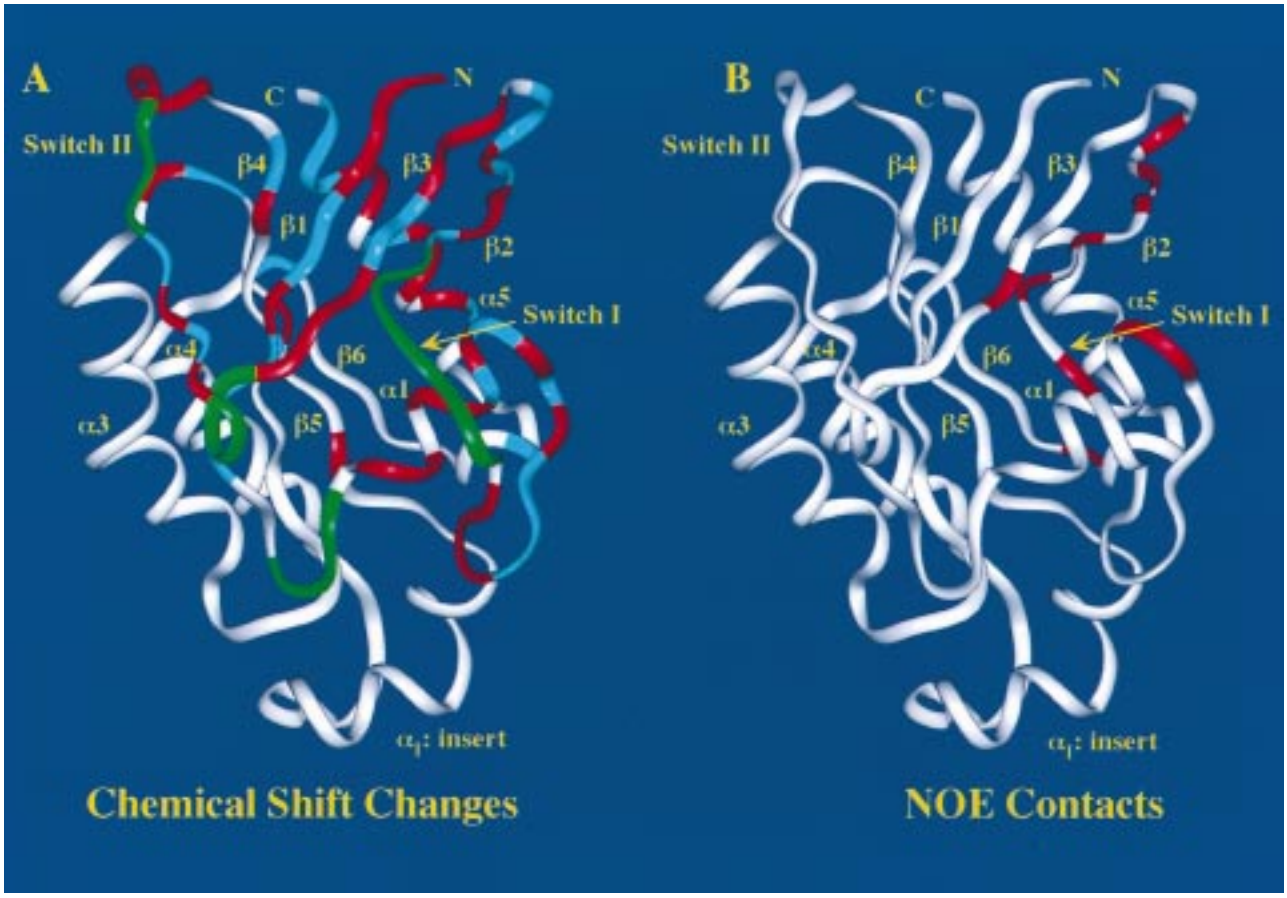

FIGURE 4: (A) The structure of Cdc42Hs·GDP (*27*) colored to indicate the chemical shift changes upon binding of PBD46. Large chemical shift changes (absolute value of the weighted average of the chemical shift change from Figure 3 is greater than 0.5) are shown in red and smaller changes (absolute value of the weighted average of the chemical shift change from Figure 3 is greater than 0.2) are shown in cyan. Residues for which there is an uncertainty are shown in green. The greatest uncertainty arises because a number of peaks in switch I are not observable in the absence of PBD46 but can be observed and assigned in the complex, thus changes in chemical shift cannot be determined. (B) The same structure colored red to indicate positions of the residues which have intermolecular NOEs to PBD46.

number of resonances exhibit significant chemical shift changes to the extent that the assignments could not be made solely upon inspection of the HSQC spectrum. The same four triple resonance experiments used for the uncomplexed form of Cdc42Hs·GMPPCP (HNCO, HNCA, HBCBCACONNH, and HNCACB) were used to assign the $^{13}C,^{15}N$-Cdc42Hs·GMPPCP-PBD46 complex. Unlike uncomplexed Cdc42Hs·GMPPCP, all resonances in switch I (residues 25−38) could be assigned in the complex. One likely explanation, consistent with the data presented below, is that interaction with PBD46 modifies the dynamics of switch I, presumably by stabilizing the structure of this region of the protein. The observed chemical shift changes (Figures 1 and 3) are extensive and map to the N-terminal half of Cdc42Hs and the α5 helix. Figure 4A indicates where on the structure of Cdc42Hs the chemical shift changes are observed.

The chemical shift changes map to the face of the protein that encompasses switch I (residues 25−38), switch II (residues 58−67), and a portion of the P-loop (residues 10−15). Thus, the binding of PBD46 might be expected to affect the binding and hydrolysis of nucleotide as well as interaction with GAP proteins [which bind to the switch I and switch II region of Cdc42Hs (*47*)]. As shown above, PBD46 inhibits GTP hydrolysis (Figure 2), and other studies have shown that it decreases the dissociation of nonhydrolyzable GTP analogues (*29*). Likewise, the original 74 amino acid construct of PBD inhibits the binding of Cdc42Hs-GAP to Cdc42Hs (*29*). Thus, the chemical shift changes are entirely consistent with the functional effects of PBD46. In contrast, the binding of RBD to H-Ras does not modify the GTPase activity of H-Ras (*48*). Likewise, the structure of Rap1, a Ras antagonist, bound to RBD (*24*) is identical to the structure of H-Ras, suggesting that RBD does not produce a structural change in H-Ras upon binding. Thus, the interaction of PBD46 with Cdc42Hs is qualitatively different than the interaction of RBD with H-Ras.

Identification of the Binding Surface on Cdc42Hs. Chemical shift changes indicate where the chemical environment is modified upon binding PBD46. Although the changes often map to the binding interface, other regions of the protein experiencing conformational changes upon binding may also exhibit changes in chemical shift. For this reason, a more precise method of mapping the interface is to measure intermolecular NOE interactions (*49*). A fully deuterated ^{15}N-Cdc42Hs·GMPPCP sample was purified in H_2O-containing buffers and complexed with natural abundance PBD46. During the purification procedure, protons were exchanged back onto the amides, providing a Cdc42Hs sample with deuterons on the carbons and protons on the amides. A three-dimensional $^{1}H,^{15}N$-NOESY-HSQC can then be used to detect NOE interactions between amide protons within Cdc42Hs and, more importantly, intermolecular NOE interactions between Cdc42Hs and PBD46. In a $^{1}H,^{15}N$-NOESY-HSQC spectrum of uncomplexed $^{2}H,^{15}N$-

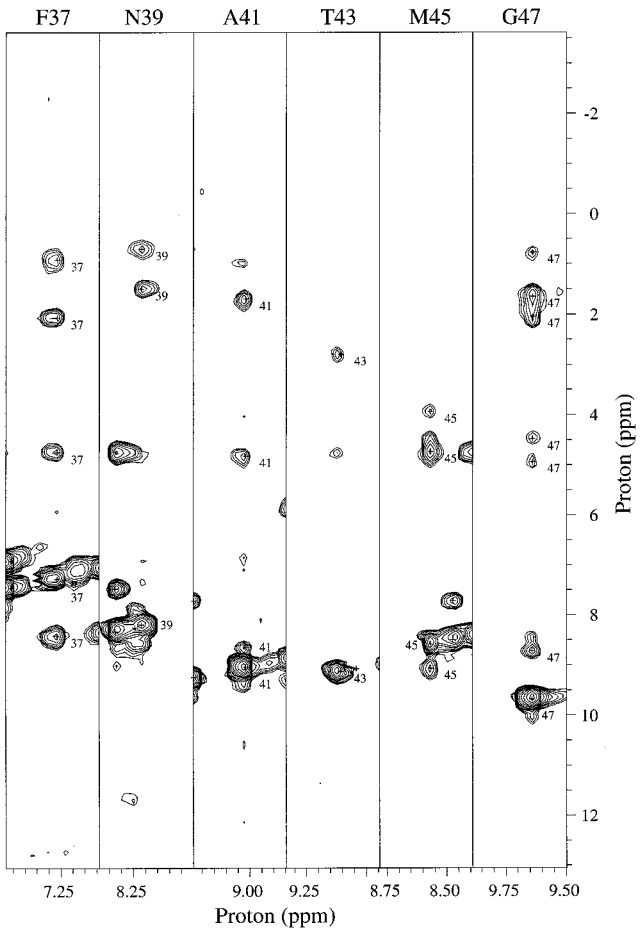

FIGURE 5: Slices from a 3D $^{1}H,^{15}N$-NOESY-HSQC spectrum of $^{15}N,^{2}H$-Cdc42Hs·GMPPCP complexed with natural abundance PBD46. Since all protons attached to carbon were replaced by deuterons, all upfield NOE peaks (>6 ppm, with the exception of NOEs to water at 4.75 ppm) are intermolecular NOEs from amide protons on Cdc42Hs to protons attached to carbon on PBD46.

Cdc42Hs·GMPPCP, the only NOE peaks observed were those between amide protons. Thus, in the complex, NOEs from nonamide protons to amide protons on Cdc42Hs arise from the dipolar interactions across the binding interface, and thus, can be used to map the binding surface. Several slices from a three-dimensional $^{1}H,^{15}N$-NOESY-HSQC spectrum are shown in Figure 5. One of the most striking features is that every other backbone amide proton from residue 37 to residue 47 of Cdc42Hs exhibits an intermolecular NOE, suggesting that a portion of the binding surface arises from an intermolecular β-sheet formed along β2 of Cdc42Hs. In addition, the interactions continue into switch I and are present in several neighboring residues in the α5-helix (Figure 4B).

These data are entirely consistent with the mutagenesis work on the binding interface between Cdc42Hs and PAK. Lamarche et al. (*50*) demonstrated that a Y40C mutation of the constitutively active Q61L mutant of Cdc42Hs abolished binding of $p65^{PAK}$ but that the F37A mutant of the same protein had no affect on the interaction. Likewise, Leonard et al. (*51*) showed that a D38E mutant of Cdc42Hs significantly weakened the binding of PAK. On the basis of the pattern of intermolecular NOEs and assuming an intermolecular β-sheet, the side chains of residues 38 and 40 face (and possibly interact with) PBD, whereas, the side chain of residue 37 points away from the interface with PBD. Thus, mutations of critical residues facing PBD at the interface would be expected to interfere significantly with the binding interaction.

This binding surface is much more extensive than that observed for the Rap1−RBD interaction (*24*). In that case, the interaction was an intermolecular antiparallel β-sheet extending from E37 to R41 of Rap1. The pattern of NOEs defining the interface suggest that an antiparallel β-sheet is also present at the Cdc42Hs−PBD46 interface, but that the β-sheet, in this case, extends for an additional six residues. These results suggest that the β2 and switch I region of Ras-like proteins may be an effector interface; however, the extent of the interface likely varies and this variation could explain the specificity of interaction and variety of functional effects observed in different members of the Ras superfamily. The indication that a number of other regions on the Cdc42Hs molecule are affected by PBD (compare panels A and B of Figures 4) raises the attractive possibility that the binding of one effector (e.g., PAK) influences the contact sites for other effectors or regulatory proteins. There is increasing evidence that the signaling activities mediated by small GTP-binding proteins require multiple effector interactions and probably occur within multicomponent complexes (*7*). Thus, the ability of one effector (PAK) to influence the binding of other effectors could provide a mechanism for coordinating multiple signaling pathways emanating from a single G-protein. Future work will be directed toward extending these observations to establish whether PAK influences specific effector interactions and what the biological consequences might be for such types of interplay.

ACKNOWLEDGMENT

The authors would like to thank Volker Dötsch, Gerhard Wagner (Harvard Medical School), Joanna Feltham (University of Massachusetts), Shubha Bagrodia, Tyzoon Nomanbhoy, Rob McFeeters, Linda Nicholson, and Greg Weiland (Cornell University) for helpful advice and assistance.

REFERENCES

1. Hall, A. (1990) *Science 249*, 635−640.
2. Ridley, A. J. (1995) *Curr. Biol. 5*, 710−712.
3. Vojtek, A. B., and Cooper, J. A. (1995) *Cell 82*, 527−529.
4. Chant, J., and Stowers, L. (1995) *Cell 81*, 1−4.
5. Qiu, R.-G., Abo, A., McCormick, F., and Symons, M. (1997) *Mol. Cell Biol. 17*, 3449−3458.
6. Hart, M. J., Eva, A., Evans, T., Aaronson, S. A., and Cerione, R. A. (1991) *Nature 354*, 311−314.
7. Cerione, R. A., and Zheng, Y. (1996) *Curr. Opin. Cell Biol. 8*, 216−222.
8. Lin, R., Bagrodia, S., Cerione, R., and Manor, D. (1997) *Curr. Biol. 7*, 794−797.
9. Zheng, Y., Bagrodia, S., and Cerione, R. A. (1994) *J. Biol. Chem. 269*, 18727−18730.
10. Aspenstrom, P., Lindberg, U., and Hall, A. (1996) *Curr. Biol. 6*, 70−75.
11. Hart, M. J., Callow, M. G., Souza, B., and Polakis, P. (1996) *EMBO J. 15*, 2997−3005.
12. McCallum, S. J., Wu, W. J., and Cerione, R. A. (1996) *J. Biol. Chem. 271*, 21732−21737.
13. Yang, W., and Cerione, R. A. (1997) *J. Biol. Chem. 222*, 24819−24824.
14. Manser, E., Leung, T., Salihuddin, H., Tan, L., and Lim, L. (1993) *Nature 363*, 364−367.

15. Manser, E., Leung, T., Salihuddin, H., Zhao, Z., and Lim, L. (1994) *Nature 367*, 40−46.
16. Bagrodia, S., Taylor, S., Creasy, C., Chernoff, J., and Cerione, R. A. (1995) *J. Biol. Chem. 270*, 22731−22737.
17. Minden, A., Lin, A., Claret, F. X., Abo, A., and Karin, M. (1995) *Cell 81*, 1147−1157.
18. Martin, G. A., Bollag, G., McCormick, F., and Abo, A. (1995) *EMBO J. 14*, 1970−1978.
19. Zhang, S., Han, J., Sells, M. A., Chernoff, J., Knaus, U. G., Ulevitch, R. J., and Bokoch, G. M. (1995) *J. Biol. Chem. 270*, 23934−23936.
20. Coso, O. A., Chiariello, M., Yu, J. C., Teramoto, H., Crespo, P., Xu, N., Miki, T., and Gutkind, S. (1995) *Cell 81*, 1137−1146.
21. Bagrodia, S., Derigard, B., Davis, R. J., and Cerione, R. A. (1995) *J. Biol. Chem. 270*, 27995−27998.
22. Ottilie, S., Miller, P. J., Johnson, D. I., Creasy, C. L., Sells, M. A., Bagrodia, S., Forsburg, S. L., and Chernoff, J. (1995) *EMBO J. 14*, 5908−5919.
23. Buday, L., and Downward, J. (1993) *Cell 73*, 611−620.
24. Nassar, N., Horn, G., Herrmann, C., Scherer, A., McCormick, F., and Wittinghofer, A. (1995) *Nature 375*, 554−560.
25. Burbelo, P. D., Drechsel, D., and Hall, A. (1995) *J. Biol. Chem. 270*, 29071−29074.
26. Shinjo, K., Koland, J. G., Hart, M. J., Narasimhan, V., Johnson, D. I., Evans, T., and Cerione, R. A. (1990) *Proc. Natl. Acad. Sci. U.S.A. 87*, 9853−9857.
27. Feltham, J. L., Dötsch, V., Raza, S., Manor, D., Cerione, R. A., Sutcliffe, M. J., Wagner, G., and Oswald, R. E. (1997) *Biochemistry 36*, 8755−8766.
28. Muchmore, D. C., McIntosh, L. P., Russell, C. B., Anderson, D. E., and Dahlquist, F. W. (1989) in *Methods in Enzymology* (Oppenheimer, N. J., and James, T. L., Eds.) pp 44−73, Academic Press, Inc., San Diego.
29. Leonard, D. A., Satoskar, R. S., Wu, W. J., Bagrodia, S., Cerione, R. A., and Manor, D. (1997) *Biochemistry 36*, 1173−1180.
30. Bradford, M. M. (1976) *Anal. Biochem. 72*, 248−254.
31. John, J., Sohmen, R., Feurstein, J., Linke, R., Wittinghofer, A., and Goody, R. S. (1990) *Biochemistry 29*, 6058−6065.
32. Nomanbhoy, T. K., Leonard, D. A., Manor, D., and Cerione, R. A. (1996) *Biochemistry 35*, 4602−4608.
33. States, D. J., Haberkorn, R. A., and Ruben, D. J. (1982) *J. Magn. Reson. 48*, 286−292.
34. Marion, D., Driscoll, P. C., Kay, L. E., Wingfield, P. T., Bax, A., Gronenborn, A., and Clore, G. M. (1989) *Biochemistry 28*, 6150−6156.
35. Bodenhausen, G., and Ruben, D. J. (1980) *Chem. Phys. Lett. 69*, 185−189.
36. Yamazaki, T., Lee, W., Revington, M., Mattiello, D. L., Dahlquist, F. W., Arrowsmith, C. H., and Kay, L. E. (1994) *J. Am. Chem. Soc. 116*, 6464−6465.
37. Kupce, E., and Wagner, G. (1995) *J. Magn. Reson., Ser. B 109*, 329.
38. Kupce, E., and Freeman, R. (1996) *J. Magn. Reson., Ser. A 118*, 299.
39. Matsuo, H., Kupce, E., Li, H., and Wagner, G. (1996) *J. Magn. Reson., Ser. B 113*, 91.
40. Yamazaki, T., Lee, W., Arrowsmith, C. H., Muhandiram, D. R., and Kay, L. E. (1994) *J. Am. Chem. Soc. 116*, 11655−11666.
41. Grzesiek, S., and Bax, A. (1992) *J. Am. Chem. Soc. 114*, 6291−6293.
42. Grzesiek, S., and Bax, A. (1992) *J. Magn. Reson. 99*, 201−207.
43. Muhandiram, D. R., and Kay, L. E. (1994) *J. Magn. Reson. 103*, 203−216.
44. Fesik, S., and Zuiderweg, E. R. P. (1988) *J. Magn. Reson. 78*, 588−593.
45. Kay, L. E., Keifer, P., and Saarinen, T. (1992) *J. Am. Chem. Soc. 114*, 10663−10665.
46. Bartels, C., Xia, T.-H., Billeter, M., Guntert, P., and Wüthrich, K. (1995) *J. Biomol. NMR 6*, 1−10.
47. Rittinger, K., Walker, P. A., Eccleston, J. F., Smerdon, S. J., and Gamblin, S. J. (1997) *Nature 389*, 758−762.
48. Herrmann, C., Martin, G. A., and Wittinghofer, A. (1995) *J. Biol. Chem. 270*, 2901−2905.
49. Walters, J. K., Matsuo, H., and Wagner, G. (1997) *J. Am. Chem. Soc. 119*, 5958−5959.
50. Lamarche, N., Tapon, N., Stowers, L., Burbelo, P. D., Aspenström, P., Bridges, T., Chant, J., and Hall, A. (1996) *Cell 87*, 519−529.
51. Leonard, D., Hart, M. J., Platko, J. V., Eva, A., Henzel, W., Evans, T., and Cerione, R. A. (1992) *J. Biol. Chem. 267*, 22860−22868.
52. Wishart, D. S., Sykes, B. D., and Richards, R. M. (1991) *J. Mol. Biol. 222*, 311−333.

BI981352+